Environmental Science & Technology

Article

pubs.acs.org/est

Photodegradation of Secondary Organic Aerosol Particles as a Source of Small, Oxygenated Volatile Organic Compounds

Kurtis T. Malecha and Sergey A. Nizkorodov*

Department of Chemistry, University of California, Irvine, California 92697, United States

Supporting Information

ABSTRACT: We investigated the photodegradation of secondary organic aerosol (SOA) particles by near-UV radiation and photoproduction of oxygenated volatile organic compounds (OVOCs) from various types of SOA. We used a smog chamber to generate SOA from α-pinene, guaiacol, isoprene, tetradecane, and 1,3,5-trimethylbenzene under high-NO_x, low-NO_x, or ozone oxidation conditions. The SOA particles were collected on a substrate, and the resulting material was exposed to several mW of near-UV radiation ($\lambda \sim$ 300 nm) from a light-emitting diode. Various OVOCs, including acetic acid, formic acid, acetaldehyde, and acetone were observed during photodegradation, and their SOA-mass-normalized fluxes were estimated with a Proton Transfer Reaction Time-of-Flight Mass Spectrometer (PTR-ToF-MS). All the SOA, with the exception of guaiacol SOA, emitted OVOCs upon irradiation. Based on the measured OVOC emission rates, we estimate that SOA particles would lose at least ~1% of their mass over a 24 h period during summertime conditions in Los Angeles, California. This condensed-phase photochemical process may produce a few Tg/year of gaseous formic acid, the amount comparable to its primary sources. The condensed-phase SOA photodegradation processes could therefore measurably affect the budgets of both particulate and gaseous atmospheric organic compounds on a global scale.

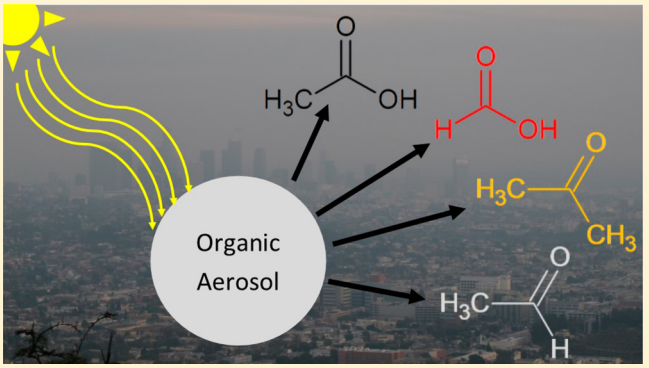

INTRODUCTION

Aerosols directly affect climate by scattering and absorbing solar radiation and by modifying cloud properties.[1] Organic compounds represent the major aerosol component, occurring in comparable amounts to sulfates, nitrates, and other major inorganic species.[2] Primary organic aerosols (POA) are emitted directly by their sources, whereas secondary organic aerosols (SOA) are produced by atmospheric reactions of volatile organic compounds (VOCs) with oxidants.[2] Various atmospheric processes involving organic aerosols (OA) and their components remain poorly understood, in part due to their complex chemical composition. A randomly selected OA particle could contain thousands of different compounds.[3]

Aging of an aerosol involves a change in composition and physical properties through various chemical and physical processes.[3] It is commonly assumed that the formation and chemical aging of SOA is driven by gas-to-particle uptake of low-volatility organics and by reactive uptake of oxidants by the particles' surfaces, with little, if any, chemistry occurring inside the particles. Recent evidence suggests that aging processes occurring in the condensed organic phase may be just as important.[3,4] The condensed-phase photochemical reactions may not only change the SOA composition, but also change the volatility distribution of the SOA compounds resulting from photoinduced fragmentation of SOA compounds into more volatile products.[5] Indeed, a recent modeling study by Hodzic et al.[6] showed that inclusion of condensed-phase photolysis in a GEOS-Chem model can potentially result in ~50% of particle mass loss after 10 days of aging. This estimate is probably too high because Hodzic et al. made an unrealistic assumption that condensed-phase photolysis of organics occurs at the same rate as in the gas-phase, disregarding matrix effects on photolysis. Absorption coefficient measurements of different types of SOA also suggested that lifetimes of SOA with respect to condensed-phase photochemistry could be quite short—assuming that every absorbed photon leads to a chemical reaction.[7] SOA mass loss and decreases in particle size due to UV irradiation have been experimentally observed in several laboratory studies.[5,8−12]

One way to study condensed-phase photochemical reactions in SOA particles is through irradiation of a model SOA prepared in a smog chamber or a flow reactor.[8] However, a potential issue with this approach is the difficulty of separating condensed-phase photochemical processes in particles from gas-phase photochemistry of volatile organics surrounding the particles. A way to more selectively study condensed-phase photochemical aging is to do experiments with bulk SOA

Received: May 9, 2016
Revised: August 21, 2016
Accepted: August 22, 2016
Published: August 22, 2016

DOI: 10.1021/acs.est.6b02313
Environ. Sci. Technol. 2016, 50, 9990−9997

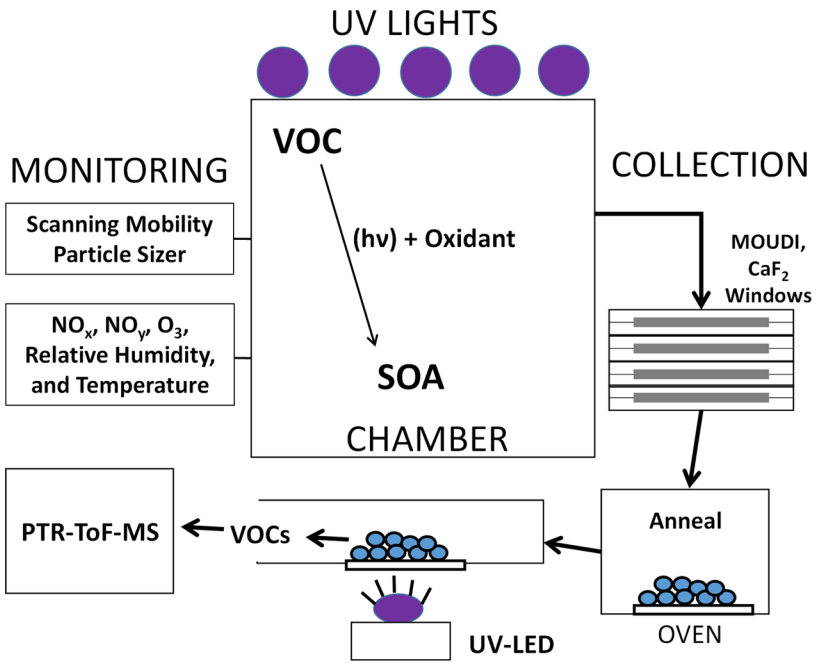

Figure 1. A diagram of SOA photodegradation experiments. The SOA is prepared in the chamber and monitored with the instruments on the left of the diagram. After a maximum particle concentration is achieved, the particles are collected, annealed, and thereafter irradiated with a UV-LED directly on the substrate. The resulting OVOCs are monitored with the PTR-ToF-MS.

material after driving away the volatile constituents,[13−15] for example, by depositing the SOA particles onto an inert substrate and carrying out UV irradiation directly on the substrate. This method offers a key advantage in that the photochemistry of gas-phase species (such as oxidant precursors and volatile organics present in chamber experiments) no longer interferes with the condensed-phase photochemistry occurring inside the SOA particles. A disadvantage of this method is that it can suffer from mass-transfer limitations during photolysis. Specifically, the time for the primary volatile products of photolysis to evaporate from the organic film (typical thickness >10 μm) may be too long compared to that for an isolated aerosol particle (typical diameter <0.5 μm), and as a result, the primary volatile products of photolysis may undergo secondary photochemical reactions before having a chance to escape from the film. For example, formic acid may actually be one of these secondary photoproducts, as suggested by Vlasenko et al.[16] In addition, the bulk film may be more depleted of oxygen during irradiation compared to aerosol particles. Previous experiments of this type in our laboratory demonstrated that condensed-phase photochemistry of SOA at λ > 295 nm produced formic acid, formaldehyde, and many other compounds, but we have not attempted to quantify the rate of photodegradation.[13−15] Related experiments by Hung et al.[17] found a significant effect of 254 nm radiation on SOA prepared from isoprene and α-pinene. To the best of our knowledge, photodegradation of other types of SOA has not been studied, and the kinetics of these processes have not yet been investigated.

The rate and extent of SOA material photodegradation can be evaluated indirectly from the amount of selected volatile products produced by the photodegradation. For example, carbon monoxide is a convenient tracer of photolysis of carbonyls.[15] In this study, we focus on the photochemical production of several oxygenated VOCs (OVOCs), including formic acid, acetic acid, acetaldehyde, and acetone in the photodegradation of different types of SOA. We find that these OVOCs are produced for a range of SOA types. We estimate that the SOA particles lose at least 1% of their mass per day under representative atmospheric conditions. Although the mass loss rate is modest, this photodegradation process can measurably affect the chemical composition of both particulate and gaseous components of aging SOA.

EXPERIMENTAL SECTION

An overview of the experimental methods is shown in Figure 1. SOA was generated in a ∼ 5 m^3 Teflon chamber in the absence of seed particles. The SOA formation was tracked with a scanning mobility particle sizer (SMPS; TSI model 3936), an NO_y monitor (Thermo Scientific model 42i-Y), an ozone monitor (Thermo Scientific model 49i), and, for selected experiments, a Proton Transfer Reaction Time-of-Flight Mass Spectrometer (PTR-ToF-MS; Ionicon model 8000).

Before SOA generation, the chamber walls were cleaned by exposure to high levels of OH and O_3 in humidified air to promote oxidation/removal of remaining species on the walls of the chamber and thereafter flushed with purge air. For a given experiment, the oxidants or their precursors were then added to the chamber; H_2O_2 served as an OH precursor in low NO_x and high NO_x photooxidation experiments; O_3 was used as an oxidant in dark experiments. The hydrogen peroxide was added by evaporating a measured volume of 30 wt % H_2O_2 solution from a glass trap under a stream of purge air at a rate of ∼10 slm (standard liters per minute), NO was added from a premixed gas cylinder, and O_3 was added by passing oxygen through a commercial ozone generator. The VOC, which served as the SOA precursor, was injected into the chamber by evaporation into a flow of air, via the same method as H_2O_2. Ideally, these experiments should have probed a range of VOC mixing ratios to examine the effect on SOA photochemistry; however, for this exploratory study, we had to use relatively high VOC concentrations, listed in Table 1, in order to collect

DOI: 10.1021/acs.est.6b02313
Environ. Sci. Technol. 2016, 50, 9990−9997

Table 1. Summary of the SOA Samples Prepared in This Work[a]

precursor	oxidant(s)	no. of repeat samples	precursor (ppm)	H_2O_2 (ppm)	NO (ppb)	O_3 (ppm)	reaction time (h)	collection time (h)
APIN	OH, low NO_x	4	1	5	0	0	3	4
APIN	OH, high NO_x	5	1	5	400	0	3	3
APIN	O_3	4	0.5	0	0	3	1	6
GUA	OH, low NO_x	3	0.5	2	0	0	3	4
GUA	OH, high NO_x	3	0.5	2	400	0	3	4
ISO	OH, low NO_x	6	3	18	0	0	5	2.5
ISO	OH, high NO_x	5	2	12	600	0	3	4
ISO	O_3	3	4	0	0	4.5	2	3
TET	OH, low NO_x	6	1	8	0	0	5	2.5
TET	OH, high NO_x	4	0.5	4	600	0	0.5	3.5
TMB	OH, low NO_x	2	0.5	4	0	0	3	3
TMB	OH, high NO_x	2	0.5	4	0	0	3	1

[a]The precursors correspond to "APIN" = α-pinene, "GUA" = Guaiacol, "ISO" = Isoprene, "TET" = Tetradecane, "TMB" = 1,3,5-Trimethylbenzene. The oxidants correspond to "O_3" = ozone, "OH, high NO_x" = high NO_x conditions, "OH, low NO_x" = low NO_x conditions. Columns 4-7 contain approximate starting mixing ratios of the precursors and oxidants.

sufficient amounts of SOA material for the experiments. A Teflon-coated fan mixed the precursor and oxidant(s) for several minutes before being shut off to reduce wall loss of particles. UV−B lamps (centered at 310 nm; FS40T12/UVB, Solar Tec Systems, Inc.) were turned on for all experiments, except for those performed with ozone as the oxidant. The aerosol was allowed to form for 1−5 h (until a maximum particle mass concentration was achieved) before the collection. Table 1 lists the conditions used in all the experiments.

SOA was collected with a Micro Orifice Uniform Deposit Impactor (MOUDI, MSP Corp. model 110-R) equipped with custom-made metal supporting rings to accommodate the uncoated CaF_2 windows as substrates instead of Teflon or foil filters. We typically collected hundreds of micrograms of SOA material per window; the largest amount was typically found on stage 7 of the MOUDI (0.32−0.56 μm particle size range). The window was then placed in a laboratory oven overnight at 40 °C with ∼10 slm of purge air flowing over it in order to drive off higher volatility species and anneal the collected SOA particles into a more uniform film on the window. The typical material loss during this process was a few percent of the collected total mass, as verified by weighing with a Sartorius ME5-F microbalance (1 μg precision).

The window was then placed into a custom-made glass flow cell with 550 sccm (standard cubic centimeters per minute) of purge air flowing over the window. A UV-light emitting diode (QPhotonics, Inc. model UVClean 300−15) with a wavelength centered at ∼300 nm, a full width half-maximum of ∼10 nm, and a power of ∼3 mW at 0.8 A current (measured with a Coherent Powermax PS19Q power sensor) was used to irradiate the particles on the CaF_2 window. The actual spectral flux density experienced by the SOA sample was also measured using actinometry as described by Bunce et al.[18] The actinometry and direct power measurements agreed with each other within a factor of 2.

The OVOCs resulting from the SOA photodegradation were detected with a PTR-ToF-MS (drift tube voltage of 600 V, field strength of ∼120 Td, drift temperature 60 °C and resolving power of $m/\Delta m \sim 5 \times 10^3$). The OVOC mixing ratios in the air flowing over the irradiated sample were estimated using the built-in calculations of the PTR-ToF-MS Viewer software from Ionicon Analytik (v.3.1.0.31), transmission curves created from a calibrated "TO-14" aromatics mix (Linde), and rate constants between the hydronium ion and the OVOCs from Zhao and Zhang.[19] In order to verify the mixing ratios estimated by this method, a calibration of the PTR-ToF-MS was later performed for selected OVOCs. Details are given in the Supporting Information (SI) (Figure S1 and Table S1).

RESULTS AND DISCUSSION

The result of a typical SOA irradiation experiment is shown in Figure 2 for an ISO/O_3 SOA sample, in which formic acid, acetic acid, acetaldehyde, and acetone are tracked by PTR-ToF-MS as a function of time. The window was inserted into the flow cell, and the UV-LED was turned on once the measured OVOC levels reached a steady state. Without the SOA sample annealing process, in which the more volatile components of SOA evaporated before the experiment, the background OVOC levels were significantly higher, and it took a long time (many hours) to achieve the steady state. In this figure, the window was placed in the flow cell just before the 0 min mark, and the irradiation began around 20 min. The resulting OVOCs were then allowed to reach a steady state count, which happened around 115 min for this run. Then the UV-LED was turned off and the counts were monitored until a baseline steady state was reached again for the next sample to be analyzed. Note that it took considerably less time for the acetaldehyde and acetone to reach the steady state levels compared to the acids, and less time to decay back to the background level. This is due to the

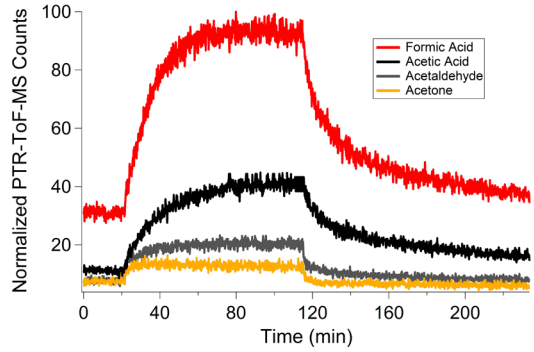

Figure 2. A time profile of the PTR-ToF-MS run for the photoproduction of various VOCs from the ISO/O_3 SOA system. The UV-LED was turned on at 20 min and turned off at 115 min in this example.

DOI: 10.1021/acs.est.6b02313
Environ. Sci. Technol. 2016, 50, 9990−9997

acids' sticky nature toward the walls of the flow cell and PTR-ToF-MS inlet line.

A number of peaks increased in the mass spectra of irradiated SOA; the list of the nominal masses of the peaks that increased the most can be found in SI Table S2. We focused our attention on the formic acid, acetic acid, acetaldehyde, and acetone peaks because of their efficient photoproduction in all the samples (with the exception of GUA SOA) and because these peaks could be assigned with a relatively high degree of confidence. We note that these were also the major OVOCs observed in photodegradation of limonene ozonolysis SOA by CIMS.[14] The assignments for many other observed peaks in the PTR-ToF-MS spectra were more ambiguous, especially at higher m/z values, as demonstrated in SI Table S3 for APIN/O_3 SOA. Because of the fragmentation in PTR-ToF-MS, we cannot exclude the possibility that fragments from larger photoproducts contributed to the observed peaks of formic acid, acetic acid, acetaldehyde, and acetone; the amounts reported below could, therefore, be overestimated. Finally, we cannot exclude the possibility that multiple structural isomers could contribute to peaks at m/z 61.028 (acetic acid, glycolaldehyde or methyl formate) and m/z 59.049 (acetone, propanal or allyl alcohol).

Numerous controls were tested with these experiments. In order to verify that OVOCs were emitted in a photoinduced process and not as a result of evaporation from the SOA material, the window was heated to a higher temperature than what resulted from the exposure to the UV-LED radiation. The sample was irradiated at λ = 310 nm and separately at λ > 450 nm using a Xe-Arc lamp (Oriel PhotoMax 60100 housing and Oriel 6256 150 W lamp with a resulting output of ∼1−6 mW) with the selected wavelength isolated with a monochromator (Oriel Cornerstone 74000) to ensure that this process required near-UV radiation. Irradiation of a blank window (exposed to purge air in the MOUDI instead of the SOA) was performed to verify that no OVOCs came from contaminations in the MOUDI or the CaF_2 windows. Finally, we utilized a slit impactor (Sioutas, stage "D") for collection (as opposed to the MOUDI), and utilized an aerosol flow tube[20] for generation of the SOA instead of the chamber to test the level of sensitivity in the measurements to the method of generation and collection of SOA. The heating, visible wavelength irradiation, and blank window irradiation experiments did not produce any detectable OVOC emissions. The slit impactor and flow tube produced results consistent with the MOUDI-collected samples from the chamber. We note that the slit impactor samples took much longer (on the scale of many hours) to reach a steady state for counts observed in the PTR-ToF-MS. This is likely due to the impaction pattern being a thick "strip" as opposed to the more evenly dispersed material collected with the MOUDI. The thicker the SOA material is on the substrate, the longer it takes for the photoproduced OVOCs to diffuse out of the material.[21] In our experiments with ∼10 μm films of SOA material, the time scale for reaching the steady state was about 20 min (Figure 2). From Fick's law of diffusion, we estimate that for submicrometer ambient particles, the phoproducts will be able to diffuse out of submicron particles on a time scale of seconds.

The optical extinction of the SOA was measured by placing the annealed CaF_2 windows in a Shimadzu UV-2450 UV−visible spectrometer. It was found that the extinction was not correlated to counts observed in the PTR-ToF-MS. The measured extinction was likely dominated by the scattering from particles on the window, which did not contribute to photochemistry. Furthermore, not all photons absorbed by SOA can lead to VOC production because of the chemical differences between different SOA types.

Although the PTR-ToF-MS signal did not correlate with the extinction for a given SOA type, there was good correlation with the SOA mass collected on the window. Figure 3 shows

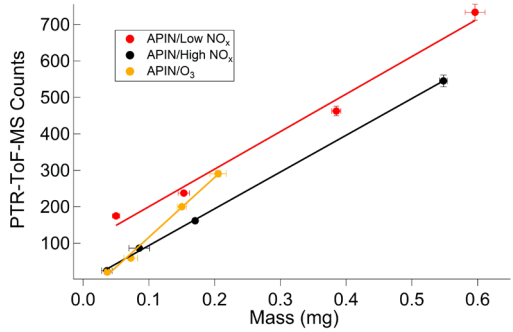

Figure 3. PTR-ToF-MS counts observed versus the mass collected for the various α-pinene SOA systems for the production of acetone. Production of other OVOCs also correlated with the mass of SOA for all the SOA samples analyzed in this study.

such correlations for the production of acetone from high-NO_x, low-NO_x, and ozonolysis SOA produced from α-pinene. Different slopes were observed for different SOA/OVOC combinations. For example, APIN/O_3 had a higher slope for the photoproduction of acetone than APIN/low NO_x and APIN/high NO_x, which is consistent with results from Romonosky et al.,[22] who studied photodegradation of different types of SOA in aqueous solutions and concluded that ozonolysis SOA are on average more photolabile than high- or low-NO_x SOA.

Because the signals observed in the PTR-ToF-MS were linearly proportional to the SOA mass across all four analyzed OVOCs and across all SOA systems (with the exception of GUA), we normalized the estimated mixing ratios of each OVOC photoproduct by the SOA mass. This normalization made it possible to compare the relative rates of OVOC production in photodegradation of different types of SOA. A plot of the resulting normalized mixing ratios is presented in Figure 4 for the four chosen OVOCs: acetaldehyde, formic acid, acetone, and acetic acid. Confidence intervals were

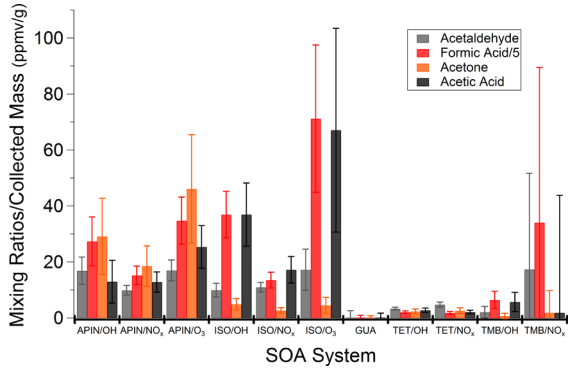

Figure 4. A bar plot showing the OVOC mixing ratios divided by the SOA mass collected for all SOA types. The error bars correspond to a 95% confidence interval range. The formic acid values are divided by 5 because its mixing ratios are much higher than for other OVOCs.

DOI: 10.1021/acs.est.6b02313
Environ. Sci. Technol. 2016, 50, 9990−9997

calculated at the 95% level which factored in the uncertainty in the mass of the SOA collected on the windows and the PTR-ToF-MS mixing ratio uncertainty. Each CaF_2 window was weighed in triplicate before and after collection of particles, and the PTR-ToF-MS uncertainty in mixing ratios employed the uncertainty in the baseline-subtracted signal and calibration factor uncertainty.

All SOA (with the exception of GUA) produced measurable amounts of OVOC photoproducts in these experiments. The relative amount of acetone photoproduct appeared to be higher for all three types of APIN SOA and lower for ISO SOA. Acetone could be a product of Norrish type-II splitting of methyl-terminated ketones, R−C(O)−CH_3, which are common among products of α-pinene oxidation.[15] Conversely, ISO SOA appeared to produce more acetic and formic acid than APIN SOA did, suggesting the secondary processes leading to these acids were more important in the ISO SOA systems. SOA from TET appeared to be less photoactive compared to SOA from APIN and ISO. SOA from saturated hydrocarbons tend to have a relatively low degree of oxidation,[23] which could contribute to their low photoactivity.

SOA from aromatic precursors TMB and GUA also produced much fewer photoproducts than SOA from APIN and ISO. In fact, guaiacol SOA did not produce any measurable OVOCs under irradiation for either high- or low NO_x SOA types. Wavelengths down to ∼250 nm (from the previously mentioned Xe-arc lamp and monochromator combination and output powers at ∼2 mW) were tested for GUA SOA photodegradation with no apparent OVOC production. This lack of OVOC production from GUA SOA and reduced OVOC production from TMB SOA is most likely due to the formation of ring-substituted products under oxidation in the chamber.[24] When these resulting products are irradiated they either form a triplet state via intersystem crossing and then form further ring substituted products (which are not volatile), or they efficiently relax.[25] Neither of these pathways provides OVOC production. Romonosky et al.[22] also noted that GUA and TMB SOA are more resistant to aqueous-phase photodegradation than other types of SOA.

The values in Figure 4 can be converted into the rate of mass loss from SOA material due to a given photoproduct. Under the steady state conditions of the experiment, the rate of production of a given molecule, rate [molec s^{-1}], can be related to the concentration of this molecule in the flow, C [molecules cm^{-3}], and the flow rate of the purge air, F = 9.17 cm^3 s^{-1}, as follows:

$$\text{rate} = F \times C \tag{1}$$

Normalizing this rate by the mass of SOA, m_{SOA} [g], and converting from concentration to volume mixing ratio, X [ppmv], and from molecules to the mass of the photoproduct, $m_{product}$ [g], yields the following expression for the fraction of SOA mass lost per unit time due to a given volatile photoproduct,

$$\frac{1}{m_{SOA}}\frac{dm_{product}}{dt} = F \times 2.46\cdot10^{13} \times \frac{MW}{N_A} \times \frac{X}{m_{SOA}} \tag{2}$$

where MW [g mol^{-1}] is the molecular mass of the photoproduct, N_A [molec mol^{-1}] is Avogadro's number, and the numeric factor (2.46×10^{13}) accounts for the unit conversion from [ppmv] to [molecules cm^{-3}] at 1 atm and 25 °C. The last term in this equation (X/m_{SOA}) is precisely the quantity plotted in Figure 4, which has a median value of ∼13 ppmv/g for all detected OVOC compounds and examined SOA types (excluding GUA). Taking the average MW of a typical OVOC photoproduct (as analyzed for this study) as 50 g mol^{-1}, the median X/m_{SOA} translates into:

$$\frac{1}{m_{SOA}}\frac{dm_{product}}{dt} = 2.4\cdot10^{-7}\ s^{-1} = 8.8\cdot10^{-4}\ h^{-1} \tag{3}$$

Based on this prediction, under the conditions of the experiment, the SOA sample would lose on average ∼0.1% of its mass after 1 h of irradiation from the UV-LED lamp as a result of a loss of a *single* volatile photoproduct. Considering that the photodegradation likely produces multiple volatile products (multiple compounds appeared in the PTR-ToF-MS spectra of the irradiated SOA, and compounds undetectable by the PTR-ToF-MS are also possible), the rate of overall mass loss could be considerably higher. To estimate the rate of the relative mass loss from SOA under ambient conditions, we can correct it by the ratio of the 24 h average integrated flux from the sun and from our UV-LED.

$$\text{factor} = \frac{\left\langle \int_{290nm}^{320nm} \text{flux}(\lambda)_{sun}\cdot d\lambda \right\rangle_{24hr}}{\int_{290nm}^{320nm} \text{flux}(\lambda)_{LED}\cdot d\lambda} \tag{4}$$

The integration extends over the wavelength where the UV-LED emits the most photons (Figure 5 compares the wavelength dependence of the UV-LED and the solar radiation). The 24 h time averaging includes both the daytime, when most photochemistry takes place, and the nighttime, when the solar flux is minimal. The solar flux was calculated at each hour using the Quick TUV calculation[26] with the following parameters: latitude/longitude = N 34° W 118° (which corresponds to Los Angeles, California), overhead ozone = 300 du, surface albedo = 0.1, ground and measured altitude = 0 km, and "pseudo-spherical discrete ordinate four streams" calculation methods. The resulting factor is 0.053 on June 20 (the summer solstice); the value is smaller for other times of the year. For example, the factor is 0.033 on April 1 (which is representative of the average earth-sun distance throughout the year).

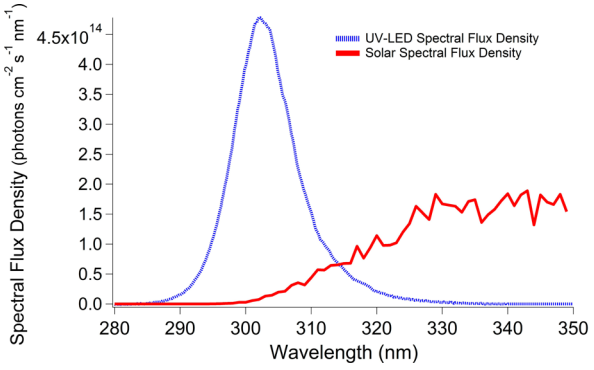

Figure 5. A plot comparing the spectral flux densities of the UV-LED and that of the sun at a solar zenith angle of 0°.

The number of OVOCs and other volatile photoproducts emitted during SOA photodegradation and detected by the PTR-ToF-MS was conservatively estimated to be $N \geq 10$ by examining the behavior of the $m/z < 100$ peaks before and during photodegradation. For example, Table S2 of the SI contains information about the top 10 peaks that increased

DOI: 10.1021/acs.est.6b02313
Environ. Sci. Technol. 2016, 50, 9990−9997

substantially upon irradiation of each SOA sample. This is a lower limit for the number of photoproducts because some of the major expected photoproducts, such as methane and carbon monoxide,[15] are not detectable by PTR-ToF-MS. If we scale the mass loss due to photoproduction of a single OVOC (eq 3) by the sun/LED factor (factor = 0.053 for June 20 in Los Angeles, California) and an estimated lower limit for the number of photoproducts (N = 10), we arrive at the conservative mass loss of at least ∼1.1% after 1 day or 7.8% after 1 week. There are not many experiments to compare this estimate to, but our result is very close to the previous observations of Epstein et al.,[8] who estimated that the mobility-equivalent diameter of APIN/O_3 aerosol decreased by 3% over a week of solar radiation (implying a ∼9% mass reduction over 1 week). Wong et al.[9] found that the mass loss rate of APIN/O_3 SOA was ∼30% after only 1 h of irradiation, which appears to be unrealistically high based on the present results. The high apparent mass loss in the Wong et al. experiments could be due to the loss of semivolatile compounds from the particles to the chamber walls or due to evaporative heating of particles by UV radiation. Despite the large spread in the existing experimental results, it is clear that the mass loss due to photodegradation could occur over atmospherically relevant time scales for a range of SOA types. SOA particles spend days in the atmosphere before they are removed; the mass loss due to the photodegradation could be significant on this time scale.

Finally, we discuss the possibility that the photochemical reactions in SOA could serve as a source of certain OVOCs. We will focus our discussion on formic acid, since it appears to be a common photoproduct for many types of SOA.[13−15] Formic acid contributes measurably to the acidity of rain and fog, particularly in remote atmospheres.[27] It is produced in the atmosphere from a variety of primary and secondary sources. Primary sources include automobile exhaust, tree emissions, and biomass burning.[28] Secondary sources include ozonolysis of alkenes and photooxidation of monoterpenes. Models do not yet account for all sources of formic acid. The emissions of formic acid in the atmosphere are currently underpredicted by up to 90 Tg yr^{-1} (out of total yearly emissions of 120 Tg yr^{-1}).[29] Stavrakou et al.[29] noted the lack of laboratory experiments utilizing monoterpenes and isoprene, two major SOA precursors, for production of formic acid. They also noted that the existing models still failed to predict the measured amount of formic acid in the atmosphere, and that a large unidentified secondary biogenic source of formic acid may exist.

To predict the global average formic acid produced per year via the process described in this paper, we used eq 2 with MW set to the molecular mass of HCOOH (46 g/mol) and the last term equal to the median X/m_{SOA} value of 106 ppmv/g for the formic values shown in Figure 4. Accounting for the sun/LED factor of eq 4, with factor = 0.033 for April 1 in Los Angeles, CA, this results in:

$$\frac{1}{m_{SOA}}\frac{dm_{HCOOH}}{dt} \times \text{factor} = 1.9\ \text{yr}^{-1} \quad (5)$$

Hodzic et al.[30] recently discussed an updated model that predicts the SOA burden in the atmosphere as m_{SOA} = 0.95 Tg. The result shows that this process can produce ∼1.8 Tg HCOOH yr^{-1}, a large value, which is close to the annual formic acid production from primary sources.[29] The photoproduction of formic acid from SOA particles could therefore contribute to the formic acid budget and help account for part of the discrepancy cited by Stavrakou et al.[29] We note that because of the potential fragmentation of larger OVOCs into the m/z corresponding to formic acid, we could overestimate its production rate from SOA. On the other hand, limiting the integration range of eq 4 only to the wavelengths over which UV-LED is emitting (290−320 nm, Figure 5) could lead to an underestimation of the production rate. Combined with the uncertainty in the PTR-ToF-MS calibration, the photoproduction rate quoted in this paper should be regarded as an order of magnitude estimate.

The results of this explarotory study show that photodegrdation of SOA can be efficieint and potentially lead to measurable mass loss from SOA particles and buildup of volatile products of SOA photodegrdation in the atmosphere. However, a number of questions have been left unaswered by this study: (a) What is the effect of relative humidity (RH) on the rate of mass loss from SOA particles? Presence of water vapor makes the SOA matrix less viscous, and this could affect the photodegradation kinetics carried out at elevated RH.[31,32] (b) What is the effect of degree of oxidation of SOA on the rate of VOC production? Molecules with a higher degree of oxidation tend to fragment more efficiently in radical driven processes,[33] and the photodegradation mechanism could be similarly affected by the SOA degree of oxidation. (c) Do photosensitized processes play any role? In our experiments, various OVOCs were emitted by the SOA film upon irradiation. Monge et al.[34] and Aregahegn et al.[35] observed an opposite process of uptake of VOCs by organic particles when an efficient photosensitizer was present on the surface. By design, our experiments could not probe the uptake resulting from such photosensitized reactions. In prelimianry experiments, in which traces of limonene or isoprene were added to the airflow over the irradiated SOA, we did not observe a significiant reduction in the limonene or isoprene mixing ratios, suggesting that our SOA samples did not contain efficieint photosensitizers. (d) What is the role of primary vs secondary photochemical reactions in the SOA matrix? (e) How does the mechanism depend on the irradiation wavelength and power? While we did not have a chance to address these and many other questions in the present study, it will be important to do these experiments in the future to better understand the effect of these processes on SOA chemistry.

■ ASSOCIATED CONTENT

Supporting Information

The Supporting Information is available free of charge on the ACS Publications website at DOI: 10.1021/acs.est.6b02313.

A description of the PTR-ToF-MS calibration for acetaldehyde, acetone, acetic acid, and formic acid; a table of PTR-ToF-MS nominal m/z values that increased the most upon UV-LED irradiation of SOA samples; and tentative peak assignments of the photoproducts of photodegradation of α-pinene ozonolysis SOA (PDF)

■ AUTHOR INFORMATION

Corresponding Author

*Phone: +1-949-824-1262; fax: +1-949-824-8671; e-mail: nizkorod@uci.edu.

Author Contributions

The manuscript was written through contributions of all authors. All authors have given approval to the final version of the manuscript.

DOI: 10.1021/acs.est.6b02313
Environ. Sci. Technol. 2016, 50, 9990−9997

Notes

The authors declare no competing financial interest.

■ ACKNOWLEDGMENTS

We thank high-school student Emily Gracheva Yen from Troy High School in Fullerton, CA for her help with the PTR-ToF-MS calibration. We acknowledge support from the U.S. National Science Foundation (NSF) grant AGS-1227579. K.T.M. thanks the NSF for support from the Graduate Research Fellowship Program. The PTR-ToF-MS was acquired with the NSF grant MRI-0923323.

■ REFERENCES

(1) Intergovernmental Panel on Climate Change. *Climate change 2013 − the physical science basis*; Cambridge University Press: Cambridge, 2014.

(2) Poschl, U. Atmospheric aerosols: composition, transformation, climate and health effects. *Angew. Chem., Int. Ed.* **2005**, *44* (46), 7520−40.

(3) George, C.; Ammann, M.; D'Anna, B.; Donaldson, D. J.; Nizkorodov, S. A. Heterogeneous photochemistry in the atmosphere. *Chem. Rev.* **2015**, *115* (10), 4218−58.

(4) Shiraiwa, M.; Yee, L. D.; Schilling, K. A.; Loza, C. L.; Craven, J. S.; Zuend, A.; Ziemann, P. J.; Seinfeld, J. H. Size distribution dynamics reveal particle-phase chemistry in organic aerosol formation. *Proc. Natl. Acad. Sci. U. S. A.* **2013**, *110* (29), 11746−50.

(5) Henry, K. M.; Donahue, N. M. Photochemical aging of α-pinene secondary organic aerosol: effects of OH radical sources and photolysis. *J. Phys. Chem. A* **2012**, *116* (24), 5932−40.

(6) Hodzic, A.; Madronich, S.; Kasibhatla, P. S.; Tyndall, G.; Aumont, B.; Jimenez, J. L.; Lee-Taylor, J.; Orlando, J. Organic photolysis reactions in tropospheric aerosols: effect on secondary organic aerosol formation and lifetime. *Atmos. Chem. Phys.* **2015**, *15* (16), 9253−69.

(7) Romonosky, D. E.; Ali, N. N.; Saiduddin, M. N.; Wu, M.; Lee, H. J.; Aiona, P. K.; Nizkorodov, S. A. Effective absorption cross sections and photolysis rates of anthropogenic and biogenic secondary organic aerosols. *Atmos. Environ.* **2016**, *130*, 172−9.

(8) Epstein, S. A.; Blair, S. L.; Nizkorodov, S. A. Direct photolysis of α-pinene ozonolysis secondary organic aerosol: effect on particle mass and peroxide content. *Environ. Sci. Technol.* **2014**, *48* (19), 11251−8.

(9) Wong, J. P.; Zhou, S.; Abbatt, J. P. Changes in secondary organic aerosol composition and mass due to photolysis: relative humidity dependence. *J. Phys. Chem. A* **2015**, *119* (19), 4309−16.

(10) Daumit, K. E.; Carrasquillo, A. J.; Sugrue, R. A.; Kroll, J. H. Effects of condensed-phase oxidants on secondary organic aerosol formation. *J. Phys. Chem. A* **2016**, *120* (9), 1386−94.

(11) Kroll, J. H.; Ng, N. L.; Murphy, S. M.; Flagan, R. C.; Seinfeld, J. H. Secondary organic aerosol formation from isoprene photooxidation. *Environ. Sci. Technol.* **2006**, *40* (6), 1869−77.

(12) Surratt, J. D.; Murphy, S. M.; Kroll, J. H.; Ng, N. L.; Hildebrandt, L.; Sorooshian, A.; Szmigielski, R.; Vermeylen, R.; Maenhaut, W.; Claeys, M.; Flagan, R. C.; Seinfeld, J. H. Chemical composition of secondary organic aerosol formed from the photooxidation of isoprene. *J. Phys. Chem. A* **2006**, *110* (31), 9665−90.

(13) Walser, M. L.; Park, J.; Gomez, A. L.; Russell, A. R.; Nizkorodov, S. A. Photochemical aging of secondary organic aerosol particles generated from the oxidation of d-limonene. *J. Phys. Chem. A* **2007**, *111* (10), 1907−13.

(14) Pan, X.; Underwood, J. S.; Xing, J. H.; Mang, S. A.; Nizkorodov, S. A. Photodegradation of secondary organic aerosol generated from limonene oxidation by ozone studied with chemical ionization mass spectrometry. *Atmos. Chem. Phys.* **2009**, *9* (12), 3851−65.

(15) Mang, S. A.; Henricksen, D. K.; Bateman, A. P.; Andersen, M. P.; Blake, D. R.; Nizkorodov, S. A. Contribution of carbonyl photochemistry to aging of atmospheric secondary organic aerosol. *J. Phys. Chem. A* **2008**, *112* (36), 8337−44.

(16) Vlasenko, A.; George, I. J.; Abbatt, J. P. Formation of volatile organic compounds in the heterogeneous oxidation of condensed-phase organic films by gas-phase OH. *J. Phys. Chem. A* **2008**, *112* (7), 1552−60.

(17) Hung, H. M.; Chen, Y. Q.; Martin, S. T. Reactive aging of films of secondary organic material studied by infrared spectroscopy. *J. Phys. Chem. A* **2013**, *117* (1), 108−16.

(18) Bunce, Nigel J.; Lamarre, Jon; Vaish, Shiv P Photorearrangement of azoxybenzene to 2-hydroxyazobenzene: a convenient chemical actinometer. *Photochem. Photobiol.* **1984**, *39* (4), 531−33.

(19) Zhao, J.; Zhang, R. Proton transfer reaction rate constants between hydronium ion (H_3O^+) and volatile organic compounds. *Atmos. Environ.* **2004**, *38* (14), 2177−85.

(20) Bones, D. L.; Henricksen, D. K.; Mang, S. A.; Gonsior, M.; Bateman, A. P.; Nguyen, T. B.; Cooper, W. J.; Nizkorodov, S. A. Appearance of strong absorbers and fluorophores in limonene-O_3 secondary organic aerosol due to NH_4^+-mediated chemical aging over long time scales. *J. Geophys. Res.* **2010**, *115*, D05203.

(21) Perraud, V.; Bruns, E. A.; Ezell, M. J.; Johnson, S. N.; Yu, Y.; Alexander, M. L.; Zelenyuk, A.; Imre, D.; Chang, W. L.; Dabdub, D.; Pankow, J. F.; Finlayson-Pitts, B. J. Nonequilibrium atmospheric secondary organic aerosol formation and growth. *Proc. Natl. Acad. Sci. U. S. A.* **2012**, *109* (8), 2836−41.

(22) Romonosky, D. E.; Laskin, A.; Laskin, J.; Nizkorodov, S. A. High-resolution mass spectrometry and molecular characterization of aqueous photochemistry products of common types of secondary organic aerosols. *J. Phys. Chem. A* **2015**, *119* (11), 2594−06.

(23) Chen, Q.; Heald, C. L.; Jimenez, J. L.; Canagaratna, M. R.; Zhang, Q.; He, L. Y.; Huang, X. F.; Campuzano-Jost, P.; Palm, B. B.; Poulain, L.; Kuwata, M.; Martin, S. T.; Abbatt, J. P. D.; Lee, A. K. Y.; Liggio, J. Elemental composition of organic aerosol: The gap between ambient and laboratory measurements. *Geophys. Res. Lett.* **2015**, *42* (10), 4182−89.

(24) Lauraguais, A.; Coeur-Tourneur, C.; Cassez, A.; Deboudt, K.; Fourmentin, M.; Choel, M. Atmospheric reactivity of hydroxyl radicals with guaiacol (2-methoxyphenol), a biomass burning emitted compound: Secondary organic aerosol formation and gas-phase oxidation products. *Atmos. Environ.* **2014**, *86*, 155−63.

(25) Turro, N. J.; Ramamurthy, V.; Scaiano, J. C. *Modern Molecular Photochemistry of Organic Molecules*; University Science Books: Sausalito, CA, 2010.

(26) Madronich, S. *Tropospheric Ultraviolet and Visible (TUV) Radiation Model*. https://www2.acom.ucar.edu/modeling/tropospheric-ultraviolet-and-visible-tuv-radiation-model (accessed August 19, 2016).

(27) Chameides, W. L.; Davis, D. D. Aqueous-phase source of formic-acid in clouds. *Nature* **1983**, *304* (5925), 427−9.

(28) Finlayson-Pitts, B. J.; Pitts, J. N. *Chemistry of the Upper and Lower Atmosphere Theory, Experiments, And Applications*; Academic Press: San Diego, CA, 2000.

(29) Stavrakou, T.; Müller, J. F.; Peeters, J.; Razavi, A.; Clarisse, L.; Clerbaux, C.; Coheur, P. F.; Hurtmans, D.; De Mazière, M.; Vigouroux, C.; Deutscher, N. M.; Griffith, D. W. T.; Jones, N.; Paton-Walsh, C. Satellite evidence for a large source of formic acid from boreal and tropical forests. *Nat. Geosci.* **2011**, *5* (1), 26−30.

(30) Hodzic, A.; Kasibhatla, P. S.; Jo, D. S.; Cappa, C.; Jimenez, J. L.; Madronich, S.; Park, R. J. Rethinking the global secondary organic aerosol (SOA) budget: stronger production, faster removal, shorter lifetime. *Atmos. Chem. Phys. Discuss.* **2015**, *15* (22), 32413−68.

(31) Lignell, H.; Hinks, M. L.; Nizkorodov, S. A. Exploring matrix effects on photochemistry of organic aerosols. *Proc. Natl. Acad. Sci. U. S. A.* **2014**, *111* (38), 13780−5.

(32) Hinks, M. L.; Brady, M. V.; Lignell, H.; Song, M.; Grayson, J. W.; Bertram, A. K.; Lin, P.; Laskin, A.; Laskin, J.; Nizkorodov, S. A. Effect of viscosity on photodegradation rates in complex secondary organic aerosol materials. *Phys. Chem. Chem. Phys.* **2016**, *18* (13), 8785−93.

(33) Kroll, J. H.; Smith, J. D.; Che, D. L.; Kessler, S. H.; Worsnop, D. R.; Wilson, K. R. Measurement of fragmentation and functionalization pathways in the heterogeneous oxidation of oxidized organic aerosol. *Phys. Chem. Chem. Phys.* **2009**, *11* (36), 8005−14.

DOI: 10.1021/acs.est.6b02313
Environ. Sci. Technol. 2016, 50, 9990−9997

(34) Monge, M. E.; Rosenørn, T.; Favez, O.; Müller, M.; Adler, G.; Abo Riziq, A.; Rudich, Y.; Herrmann, H.; George, C.; D'Anna, B. Alternative pathway for atmospheric particles growth. *Proc. Natl. Acad. Sci. U. S. A.* **2012**, *109* (18), 6840−44.
(35) Aregahegn, K. Z.; Noziere, B.; George, C. Organic aerosol formation photo-enhanced by the formation of secondary photosensitizers in aerosols. *Faraday Discuss.* **2013**, *165*, 123−34.

DOI: 10.1021/acs.est.6b02313
Environ. Sci. Technol. 2016, 50, 9990−9997